Continuous flow synthesis of functionalized silver nanoparticles using bifunctional biosurfactants

D. V. Ravi Kumar,[b] Manasi Kasture,[b] A. A. Prabhune,[c] C. V. Ramana,[d] B. L. V. Prasad*[b] and A. A. Kulkarni*[a]

Received 21st September 2009, Accepted 10th December 2009
First published as an Advance Article on the web 4th February 2010
DOI: 10.1039/b919550e

Silver nanoparticles were synthesized by continuous flow methods using biosurfactants, namely, oleic acid sophorolipid (OASL) and stearic acid sophorolipid (SASL). Both the sophorolipids can act as reducing and capping agents. The effect of temperature on the completion of nanoparticle formation and the particle growth dynamics (size) were studied in batch mode. While the completion of the reaction using oleic acid sophorolipid needed 20 min, only 5 min were required with the stearic acid sophorolipid as capping and reducing agent. Hence all the continuous flow experiments were carried out using the stearic acid sophorolipid. The continuous flow synthesis of silver nanoparticles was carried out in a stainless steel helical coil and also in a spiral polymeric minichannel reactor. The DLS results show that higher flow rate leads to the formation of bigger and polydisperse particles because of incomplete reactions. Higher residence time allowed the completion of reaction leading to spherical, small and monodisperse particles.

1. Introduction

Nanomaterials have tremendous applications in the areas like catalysis, electronics,[1] functionalized materials, coating, drug delivery, biotechnology,[2] nanofluids for heat transfer[3] *etc*. All these applications largely depend on the shape, size and functionality of the nanomaterials, and often, it is a challenge to achieve the desired shapes and sizes without significant deviation.[4,5] The size and shape of the nanomaterials is largely dependent on method of synthesis and the substrates. Thus any method of synthesis that offers a better control on the size and shape of the particles gets importance. The conventional approach of synthesis in batch process has been useful to derive new synthetic routes, studying their mechanism and for measuring the various properties of the synthesized materials, but there exist several limitations in extending the process for large scale synthesis. Some of the noticeable limitations of traditional reaction vessels include inefficient micromixing (mixing has to be in nanoscale to achieve the best results), non-uniformity of the temperature throughout the reactor, non-idealities in flow rates resulting in wider particle size distribution *etc*. Moreover thorough cleaning of the vessel is needed after every batch to avoid contamination.[6] Most of these limitations can be overcome by using microreactors for the synthesis. In the last couple of years there are many such examples where the continuous flow synthesis of the nanomaterials by using microreactors has been demonstrated. The summary of few such reports is given in Table 1.[7-19]

In addition to these, very few literature reports discuss the synthesis of different shaped nanomaterials like rods, hexagons,[20,21] *etc*. A few studies also report on the size tunability of particles[22] and synthesis of core shell type structures[23] in microreactors using continuous flow methods. The microfluidic methods have many advantages like reduced consumption of reagents, safety[24] and stoichiometric yield satisfying all the requirements of large scale preparation of nanomaterials. Above all, a high surface to volume ratio in micro channels leads to better heat and mass transfer,[25] which is useful to control the reaction rates and hence the properties of synthesized material.

Silver nanoparticles demonstrate *anti* microbial activity[26] and are widely used as SERS substrates[27] and hence it is considered as a useful model system for synthesis in microreactors.[17] In most of the reported methods the optimization of experimental parameters has not been addressed and the use of external reducing and capping agents[8,10] affects the stability of the particles, complete consumption of reactants and finally the yield of nanoparticles. Complete consumption of reactants is very important in the chemical methods of synthesis so that the methods remain feasible even at large scale. In this paper we report the continuous flow synthesis of silver nanoparticles in aqueous medium by bifunctional biosurfactants called sophorolipids which reduces silver ions in basic conditions and cap them simultaneously. This avoids the usage of an external reducing agent thereby reducing the number of reactants, which is a favorable case for continuous flow synthesis.

Sophorolipids are a class of glycolipid molecules bearing a sophorose, a dimeric glucose, attached to the ω or ω-1 carbon of fatty acids, which find many biological applications.[28,29] In

[a]*Chem. Eng. Division. (CEPD), National Chemical Laboratory, Pune, 411 008, India. E-mail: aa.kulkarni@ncl.res.in; Fax: 91 20-25902621; Tel: +91 20-25902153*
[b]*Physical Chemistry Division, National Chemical Laboratory, Pune, 411 008, India. E-mail: pl.bhagavatula@ncl.res.in; Fax: 91 20-25902636; Tel: +91 20-25902013*
[c]*Biochemical Sciences Division, National Chemical Laboratory, Pune, 411 008, India*
[d]*Division of Organic Chemistry, National Chemical Laboratory, Pune, 411 008, India*

Table 1 Summary of literature reports on continuous flow synthesis of nanoparticles

Author and Year	System Studied	Microreactor details Channel width/W, Length/L	Conditions Flow rate ~ (Q μL min^{-1}) Temperature ~ (T)	Observations Particle size (d_P)
Wagner *et al.*, 2004[7]	Metal (Au)	No details on the channel width	Q ~ 10–50 μL min^{-1}	d_P ~ 11.8–23.7 nm
Lin *et al.*, 2004[8]	Silver	L (immersed in oil bath) = 20 cm, i.d. = 0.84 mm	Q ~ 0.08–0.7 mL min^{-1} T ~ 110–140 °C	d_P ~ 8.7–5.6 nm
Khan *et al.*, 2004[9]	Colloidal Silica	L = 40 mm W = 0.05 mm followed by ageing section	Q ~ 2–20 μL min^{-1}	d_P ~ 10 nm–1μm
Kohler *et al.*, 2005[10]	Gold	W = 0.178–0.7 mm	Q ~ 0.5–8 mL min^{-1}	d_P ~ 5–50 nm
Shalom *et al.*, 2007[11]	Thiol capped Gold	W = 0.15 mm	Q ~ 0.4–0.8 mL min^{-1}	d_P ~ 2.9–4.9 nm
Yen *et al.*, 2003[12a]	CdSe	W = 0.25 mm	T ~ 180–320 °C Residence time 1-15 min	d_P ~ 3.4–5.4 nm
Kawa *et al.*, 2003[12b]	CdSe	SS tube 4.2 mm i.d.	Q ~ of TOPO is 42.4 mL min^{-1}; Cd/Se stock solution 17.6 mL min^{-1}	d_P < 10 nm
Köhler *et al.*, 2008[13]	Au–Ag	Glass channels W = 0.5–0.3 mm L = 10 mm	Q ~ 20 & 50 μL min^{-1}	Results star like core shell type Au/Ag nanoparticles, d_P ~ 80-120 nm
Köhler *et al.*, 2007[14]	Au–Ag	W ~ 0.2–0.7 mm	Q ~ 5 μL min^{-1}-5 mL min^{-1}	Metal nano particles of various composition
Lee *et al.*, 2009[15]	Iron Oxide	PDMS micromixer of Two different channels (inner and outer) of W ~ 974 and 724 μm	Q ~ 300–640 μL min^{-1}	d_P ~ 4.83–5.24 nm
Song *et al.*, 2006[16]	Co	Polymeric microfluidic reactor W ~ 150–400 μm	Q ~ 0.08, 0.9 mL min^{-1},	Different phases of Co NPs were synthesized by varying the flow rate and quenching time
He *et al.*, 2008[17]	Ag	PTFE capillary tube L = 200 cm and 0.3 mm i.d.	Q ~ 70.7, 28.2, 14.2 mL min^{-1}	d_P ~ 4.8–8.1 nm
Huang *et al.*, 2008[18]	Ag	Microreactors of three different i.d 5, 3, 0.5 mm	Q ~ 0.5–1 mL min^{-1} T ~ 90 °C	d_P ~ 10.5–23.3 nm
Abou-Hassan *et al.*, 2008[19]	Iron Oxide	Coaxial flow milli channel	Q_{in} = 100 μL min^{-1} Q_{out} = 400 μL min^{-1}	—

this study, initially, the reaction conditions were optimized in the batch process by using two different sophorolipids. The optimized parameters were then extended for the continuous process.

2. Experimental

2.1 Materials

$AgNO_3$ (SRL), KOH (Merck, Germany), oleic acid (Sigma-Aldrich) were purchased and used without any further purification. Oleic acid sophorolipid (OASL) was prepared by an already established method.[28] This oleic acid sophorolipid was further subjected to selective olefinic hydrogenation to obtain stearic acid sophorolipid (SASL).

2.2 Synthesis in batch mode

$AgNO_3$ (10^{-3} M) and sophorolipid solution (10^{-3} M, 10 mL) were mixed at room temperature and heated to 90 °C. 1 mL solution of concentrated KOH (≈ 0.005 M) (approx.) was added to this mixture at 90 °C. The mixture was constantly stirred while maintaining constant temperature using a thermostat (Julabo, Germany). The aliquots from the reaction mixture were sampled at equal time intervals and analyzed with UV-Visible spectrophotometer. The same procedure was followed for both the sophorolipids. The *anti*-bacterial activity of the silver nanoparticles synthesized by sophorolipid was explained in earlier work.[26b]

2.3 Synthesis of silver nanoparticles in stainless steel tubular microreactor

Based on the analysis from the batch experiments (Section 3), stearic acid sophorolipid was chosen as the capping and reducing agent for the continuous flow experiments. A Stainless Steel tube (SS316) of length 1 m with 1.38 mm i.d. and 1.58 mm o.d. acted as millireactor. Following the procedure mentioned previously, two solutions were made: (a) mixture of 10^{-3} M solution of $AgNO_3$ and stearic acid sophorolipid and (b) concentrated KOH solution and these were filled in 20 mL and 2 ml syringes, respectively. A dual syringe pump (Boading Longer, China) was used for driving the reactants into the micromixer and the reaction tube. The flow rate for mixture (a) was maintained at 0.272 mL min^{-1}, while the KOH solution was passed at 0.0272 mL min^{-1}. The outlets of the syringes were connected to a simple T-mixer (0.8 mm i.d.) using in-house designed and fabricated (Glass to Metal) Teflon connectors. The fluids mixed in the T-mixer subsequently entered the reaction tube. The T-mixture and the reaction tube were immersed in thermostat (Julabo, Germany) and the temperature was maintained at 90 °C. The flow rates were maintained to achieve a residence time of 5 min, which is required to complete the reaction and the samples were collected

at the outlet. The samples were immediately subjected to analysis. A schematic of the experimental set-up is shown in Fig. 1.

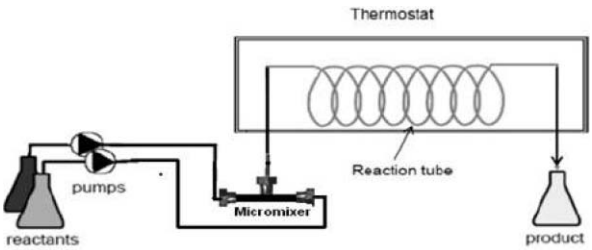

Fig. 1 Schematic Diagram of the Experimental Setup.

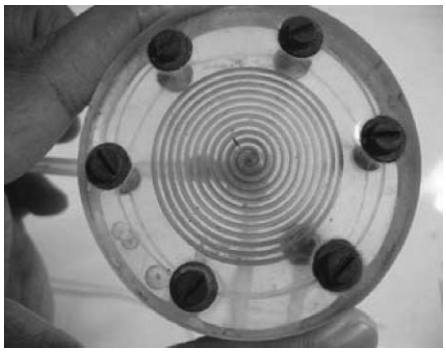

Fig. 2 Photograph of Spiral Millireactor.

2.4 Synthesis of Ag nanoparticles in spiral millireactor

For the helical coil (with i.d of the coil D, which is the case similar to the SS tubular reactor) having specific radius of curvature (Rc), the ratio of the Dean number (De) to Reynolds number (Re) is always constant and is equal to $\sqrt{D/Rc}$. During the synthesis of nanoparticles in such a geometry, where the particles grow along the length of coil/tube, the particles exhibit enhanced drag while they flow. Also, the lift force acting on the particles keeps changing its directions as the particles follow the helical path. This situation is not ideal as the pressure drop in the lower half of a vertically oriented helical coil (referring to the schematic of experimental set-up in Fig. 1) is relatively higher than the upper half and is expected to induce back mixing thereby yielding non-idealities in the particle size distribution. A similar situation would exist if the coil is oriented to have a horizontal flow, where again the fluid backmixing is known to affect the particle size distribution. One of the methods to overcome such non-idealities resulting from the geometry is to use segmented flow.[9] However presence of an inert phase reduces the active volume of the device thereby reducing the synthesis capacity. In view of this, here we propose to use a spiral microreactor, where the spiral evolves in outward direction resulting into continuous increase in the radius of curvature. Although the values of De and hence the centrifugal force would continue to decrease with increase in Rc, this kind of a geometry is expected to yield continuous development of the flow with non-parabolic velocity profile. Continuously developing skewed mean velocity profile would lead to controlled local backmixing and the extent of backmixing would thus strongly depend upon the total length of the spiral and the spatial increase in Rc. Keeping this in mind, a PMMA millireactor having a spiral channel geometry (channel width and depth of 0.5 mm, with 12 spiral rounds having pitch of 1 mm) was fabricated using conventional micro machining (Fig. 2). The possible variations of the geometry, channel sizes, angle of expansion and its effects on the performance will be discussed separately with the help of detailed flow modelling. The number of spiral turns were restricted to 12 to avoid building up of high pressure drop across the channel.

The experimental set-up was similar to the previous one except that the SS tube was replaced with the acrylic device, which was oriented to yield a horizontal flow. The experiments were performed at two different flow rates, 35 μL min^{-1} and 100 μL min^{-1}, which yield residence time of 300 s and 105 s, respectively. The samples collected at the outlet were chilled using ice thereby reducing the possibility of further reaction before characterization.

2.5 Characterization

The synthesized samples were characterized using the following techniques and the analysis results are discussed subsequently:

a. UV-Visible Spectrophotometer (Jasco-V570) with a resolution of 2 nm.

b. Samples were coated on glass plates and dried to analyze with powder X-ray diffraction (Xpert Pro, PANalytical) using Cu-Kα (1.54 A°) radiation within the range of 10–80 with the scan rate of 2.3°/min.

c. Dynamic light scattering experiments were carried out by using Brookhaven instrument model 90 Plus Particle Size Analyzer and the size distribution of particles was analyzed based on the number of particles.

d. The TEM grids were prepared by placing a drop of sample on carbon coated copper grids and analyzed with FEI model Technai G2 operated with an accelerated voltage of 300 kV. For TEM analysis, the raw sample collected directly at the tube/channel outlet and the sample subjected to centrifugation and redispersion of particles, both were used.

3. Results and discussions

The rates of nanoparticle formation and growth are a strong function of the reaction kinetics and hence of the temperature of the reaction mixture. From our earlier studies[30] we monitored the effect of temperature on the progress of reaction by the UV-Visible spectra at different temperatures. In the case of reaction conducted with OASL as the temperature increases (i.e from room temperature to 90 °C) the intensity of peak in UV-Visible spectra has also increased and it is prominent at 90 °C. At higher temperatures, because of the rapid homogeneous nucleation, most of the limiting reactant will be consumed and the growth will be diminished. This results in small and monodispersed particles.[18,31] The silver nanoparticles synthesized at 90 °C were monodispersed and smaller in size (5.5 nm) than the particles synthesized at lower temperatures (20 nm). The concentrations of the precursors were also optimized. Based on these results further experiments were carried out at 90 °C as the optimized temperature. The same procedure (mentioned in the experimental section) was followed with SASL to know the reaction completion period and also to select better reducing/capping agent which makes the reaction proceed faster. The aliquots were

taken from the reaction mixture from both the batch process experiments *i.e.* from OASL and SASL after 0, 2, 5, 8, 10, 15, 20, 25, 30, 45 min, after the reaction started. The samples were analyzed with UV-Visible spectrophotometer and the results are shown in Fig. 3 and Fig. 4. In case of OASL up to 5 min the intensity of SPR peak centered at 420 nm is very low indicating that the reaction is not complete. From 8 min onwards the SPR peak intensity gradually increases till 20 min, after which no significant change in the peak intensity is observed suggesting the completion of reaction.

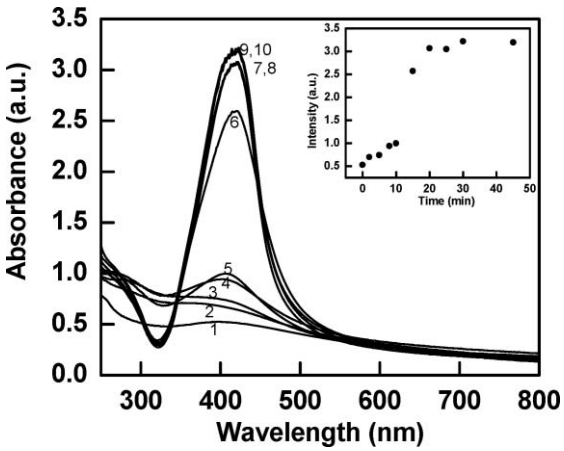

Fig. 3 Time dependent UV-Visible spectra of silver nanoparticles synthesized by oleic acid sophorolipid. Curves 1–10 show the UV-Visible spectra from 0–45 min respectively. The 420 nm peak intensity with time of reaction plotted in the inset.

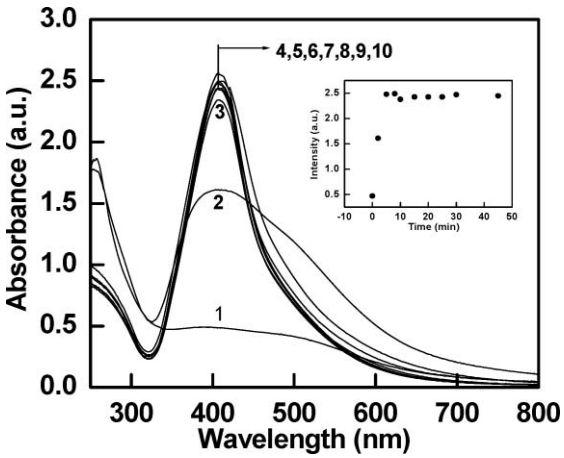

Fig. 4 Time dependent UV-Visible spectra of silver nanoparticles synthesized by stearic acid sophorolipid. Curves 1–10 show the UV-Visible spectra from 0–45 min respectively. The 420 nm peak intensity with time of reaction plotted in the inset.

The time dependent UV-Visible results from stearic acid sophorolipid experiments indicate that the silver nanoparticles formation started after 2 min (by observing the peak around 420 nm) and its absorbance increased up to 5 min after which it does not change much. The particle size distribution was measured in both the experiments after the start of the reaction and after the reaction was complete *i.e.* after 2 and 45 min.

For the case of OASL derived silver nanoparticles, the particles were polydispersed and large in size after the 45 min of the reaction (Fig. 5), while the nanoparticles synthesized from SASL were small in size and monodispersed (Fig. 6). These results correspond to the raw samples. One of the reasons that could lead to the presence of a few large size particles after 2 min of reaction (Fig. 5) is the presence of Ag-sophorolipid complex which is yet to undergo a reaction. However after 45 min, although the reaction is complete, longer time due to slow reaction in the presence of OASL may induce particle agglomeration thereby yielding a greater number of large size particles. The particles forming these agglomerates can be redispersed after post processing of samples.

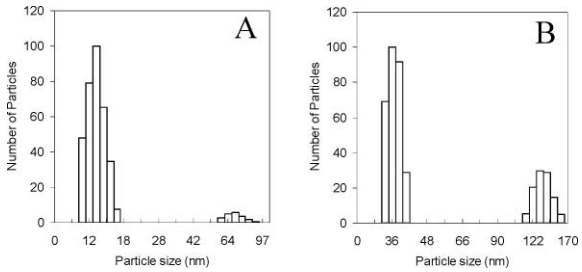

Fig. 5 Particle size distribution of silver nanoparticles synthesized from oleic acid sophorolipid after A) 2 min B) 45 min.

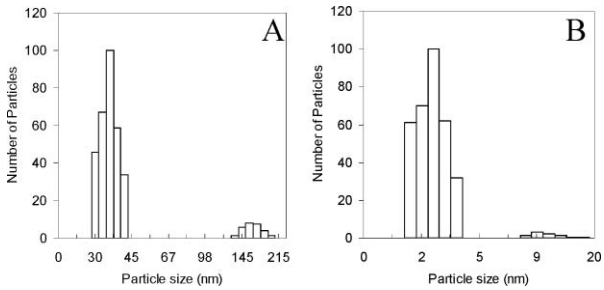

Fig. 6 Particle size distribution of silver nanoparticles synthesized with stearic acid sophorolipid after A) 2 min B) 45 min.

The difference in the time required for the completion of reaction with different sophorolipids can be explained from the structures of sophorolipids shown in Schemes 3.1 and 3.2.

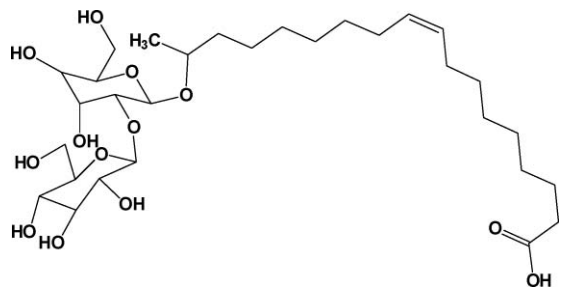

Scheme 1 Structure of oleic acid sophorolipid

The OASL has one double bond, which is absent in SASL. Since silver ions are known to bind to the olefinic double bond, in the case of OASL there is a possibility of formation of silver ion-olefin complex which hinders the reduction.[30,32] On the other hand in the absence of any double bond, no such possibility exists for the case of SASL. As a result, the reaction rates are relatively higher with SASL than with OASL as a capping and

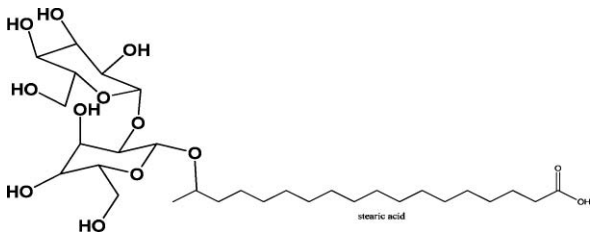

Scheme 2 Structure of stearic acid sophorolipid

reducing agent. Also, the particles were of better uniformity in size and the completion of particle formation could be achieved in a relatively shorter time (5 min). These factors helped to choose SASL for the continuous flow experiments.

The UV-Visible spectra of Ag nanoparticles synthesized by continuous flow experiments using stainless steel tubular microreactor, with a flow rate of 0.272 mL min^{-1} and a residence time of 5 min showed SPR peak of silver at 420 nm. Particle size distribution from light scattering experiment shows that the particle size was reasonably narrow with a size range of 5 to 9 nm (Fig. 7). The TEM images agree well with the trends observed from UV-vis spectra and particle size distribution results (Fig. 8). The powder X-ray diffraction pattern of the sample obtained in continuous flow reaction was similar to the pattern from the batch process result and thus confirms the formation of silver nanoparticles (Fig. 9).

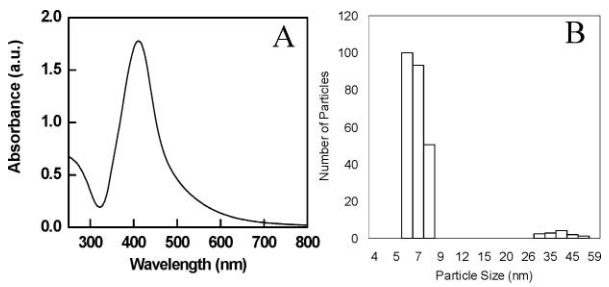

Fig. 7 A) UV-Visible Spectra and B) Particle Size distribution of Silver nanoparticles synthesized from stearic acid sophorolipid in Stainless Steel tubular microreactor with a flow rate of 0.272 mL min^{-1} for 5 min.

It is reported in the literature that the particle size distribution of the nanoparticles in continuous flow gets affected by the velocity profile in the channel. Since the flows are laminar, the velocity profile is parabolic, where in the absence of significant radial dispersion the particles in the centre spend relatively less time in the channel than those in the near wall region.

One of the ways to overcome the problem of polydispersion is the use of segmented flows as demonstrated by Khan *et al.* and Yen *et al.*[9,33] However the issue of reduced active capacity of the channel and hence the reduced throughput further needs to be resolved. In view of this, as mentioned previously, it was thought desirable to modify the flow by generating spatially varying secondary flows in addition to the convective flow. These secondary flows would help to make the particles cross the streamlines from purely convective flow thereby enhancing the uniformity in their residence time. In order to achieve this objective, as mentioned previously, we have used a spiral geometry where the secondary flows vary continuously with increasing radius of curvature. The total length of the channel was 0.7 m and the reactants enter the channel at the centre

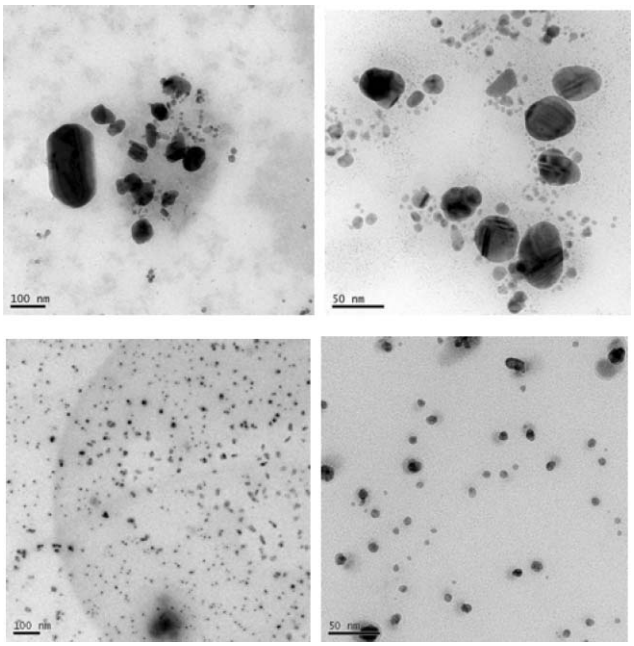

Fig. 8 TEM images of Silver nanoparticles synthesized from stearic acid sophorolipid in SS tube (1.38 mm i.d.) with a flow rate of 0.272 mL min^{-1}. (Top row) TEM images of the raw sample collected at the outlet of microreactor. (Bottom) TEM images after centrifuging (14000 rpm) and redispersion.

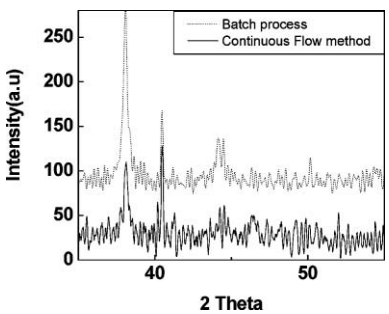

Fig. 9 X-Ray diffraction pattern of Ag nanoparticles synthesized from a) Batch process b) Continuous flow method using stainless steel tubular microreactor.

of the spiral and follow the fluid path which has increasing radius of curvature. Three different flow rates: 1 mL min^{-1}, 100 μL min^{-1} and 35 μL min^{-1} were maintained to synthesise silver nanoparticles. These flow rates yield the residence time of time of 10.5 s, 105 s and 300 s respectively.

From the UV-Visible results (Fig. 10) we observe that the peak corresponding to 100 μL min^{-1} occurs at lower wavelength (blue

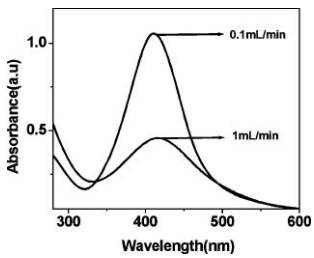

Fig. 10 UV-Visible Spectra of Ag nanoparticles synthesized from stearic acid sophorolipid in Acrylic polymer made microreactor.

shifted) and is narrow in nature. It is well known that in UV-Visible spectrum the peak at lower wave length indicates smaller particle size and a narrow peak indicates the monodispersity of the particles.[34] On the other hand, the particles synthesized at higher flow rate (1 mL min^{-1}) were larger in size. The dynamic light scattering experiment results supported this observation and shows a particle size of 8–13 nm for 100 μL min^{-1} and 50–60 nm for 1 mL min^{-1} (Fig. 11).

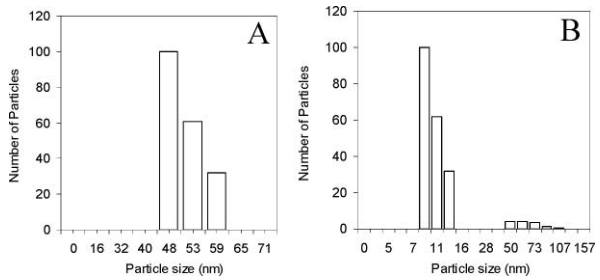

Fig. 11 Particle size distribution of Ag nanoparticles synthesized at A) 1 mL min^{-1} B) 100 μL min^{-1}.

TEM image of the particles which were synthesized at 1 mL min^{-1} clearly shows (Fig. 12) that particles are polydispersed, not well separated and some of those were bound by a low contrast material which could be attributed to the sophorolipid. It would be interesting to note that, unlike the case of a collapsing spiral geometry,[35] our approach of using the centre as inlet for the reactants leads to constant increase in the relative dominance of the convective flow over the secondary flows (due to changing *De*) which would help to keep the fluids completely mixed and thereby reduce the possibility of any deviation in the particle sizes due to the presence of axial dispersion alone as it is observed in straight channels.[9] For a given flow rate and channel diameter, the secondary flows would decrease with increasing radius of curvature. Thus, the ratio of convective to secondary flows is solely governed by the design itself. Hence, although the higher flow rates would help achieve better mixing at the cost of higher pressure drop, it yields lower residence time and hence an incomplete reaction. At lower flow rates, the system behaves more like a unidirectional plug flow as the overall secondary flows are always quantitatively very small. Thus, mixing is efficient in the portion with smaller radius of curvature followed by the section that only acts as a residence time unit with relatively slower secondary flows. Longer residence time would lead to completion of reaction and more relatively monodispersed particles than the helical SS tube of identical length (Fig. 14).

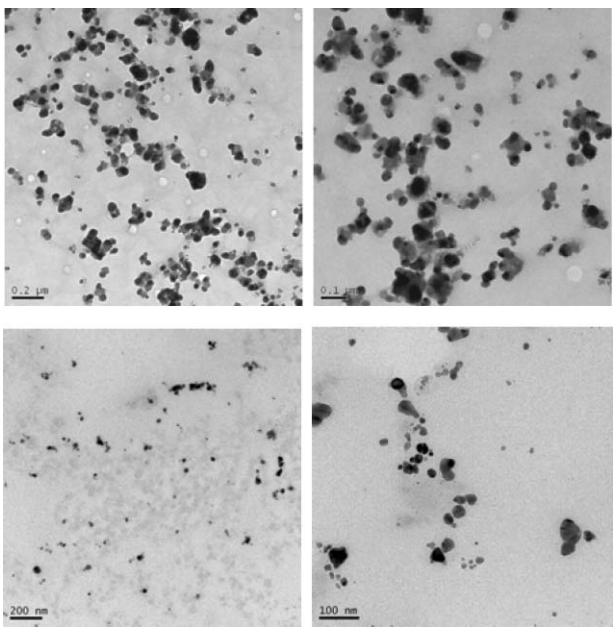

Fig. 12 Silver nanoparticles synthesized from stearic acid sophorolipid in acrylic microreactor with a flow rate of 1 mL min^{-1}. (Top row) TEM images of the raw sample collected at the outlet of microreactor. (Bottom) TEM image after centrifuging (14 000 rpm) and redispersion.

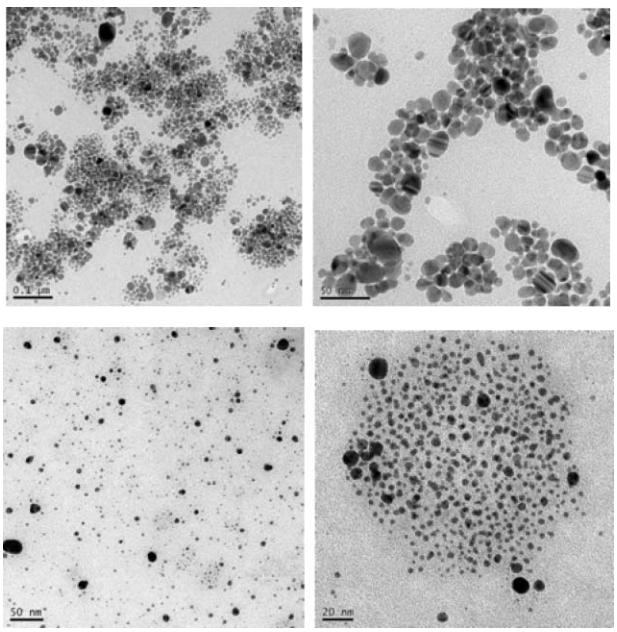

Fig. 13 TEM images of Silver nanoparticles synthesized from stearic acid sophorolipid in spiral milli reactor with a flow rate of 100 μL min^{-1}. (Top row) TEM images of the raw sample collected at the outlet of microreactor. (Bottom) TEM images after centrifuging (14 000 rpm) and redispersion.

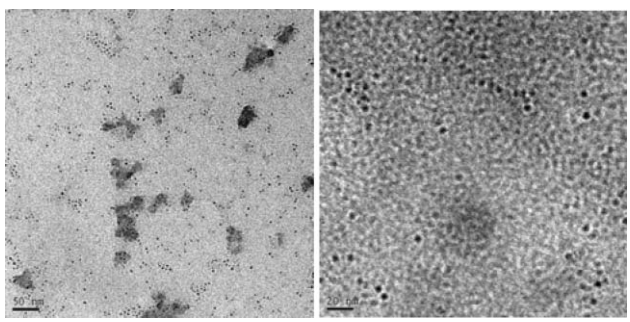

Fig. 14 Silver nanoparticles (tiny dark dots) synthesized from stearic acid sophorolipid in acrylic microreactor operated with 5 min residence time. TEM image is obtained after centrifuging and redispersion.

In case of 1 mL min^{-1} flow rate, the residence time (10.5 s) was just sufficient to initialize the nucleation and particle formation, (silver particles were observed in TEM and UV-Visible) but the reaction was incomplete and it was clearly evident from the presence of silver–sophorolipid complex in the TEM images

(Fig. 12; top row). Removal of this unreacted material showed the presence of very small particles (Fig. 12; bottom row). With higher residence time for 100 μL min^{-1} (105 s), the particles were well shaped and there was no low contrast material (sophorolipid) observed. Thus, although we could see the nucleation and initial growth of particles, this does not represent the final size distribution at the end of the reaction since the residence time was still less than the time required for completion of the reaction (Fig. 13). Here again simple centrifuging resulted in isolation of synthesized nanoparticles with narrower size distribution and they started self assembling in hexagonally close packed arrangements on the TEM grid (Fig. 13; bottom row). The observations from images also show that the particles which were synthesized at lower flow rates are smaller in size, monodispersed but tend to form clusters due to less dominance of the flow field. With further reduction in the flow rate to 35 μL min^{-1}, the residence time of 5 min was achieved and the experiments in spiral geometry led to the completion of the reaction and achieved almost spherical particles with uniform size (3–4 nm) as can be seen in Fig. 14. Presence of some amount of low contrast material indicated the presence of remnant sophorolipid. However the synthesized nanoparticles were clearly spherical and supports the role of secondary flow to attain monodispersed particles. The detailed analysis on the operational and design related issues of such devices and the quantitative role of the secondary flow on particle sizes will be evaluated by rigorous CFD simulations will be quantified and discussed separately.

4. Conclusions

The synthesis of silver nanoparticles with a biosurfactant and optimization of reaction conditions from batch process has been discussed. The synthesis in the presence of stearic acid sophorolipid was much more rapid than oleic acid sophorolipid. On the basis of the optimized conditions, the continuous flow synthesis of Ag nanoparticles was carried out in a tubular reactor and also in a spiral geometry. The observations from different characterization techniques showed that if sufficient residence time is given to complete the reaction, a spiral geometry helps to yield monodispersed spherical particles. The possible effect of axial dispersion was seen to be overcome by the induction of secondary circulatory motion in a continuously developing flow. The observations are consistent with the expected effect of flow in the device. Further experiments on inline synthesis and separation of nanoparticles and a detailed analysis of the flow are in progress and will be reported separately.

Acknowledgements

All the authors acknowledge the financial help from the Consortium on Microreaction Technology (www.ncl-india.org/cmr/) and Centre of Excellence on Microreactor Engineering of NCL. DVRK and MK thank CSIR, New Delhi for financial support. BLVP, AAP and CVR thank the DBT for financial support. CVR thanks the DST for funding through the Green Chemistry Program (No. SR/S5/GC-20/2007).

Notes and references

1 J. H. Ahn, H. S. Kim, K. J. Lee, S. Jeon, S. J. Kang, Y. G. Sun, R. G. Nuzzo and J. A. Rogers, *Science*, 2006, **314**, 1754–1757.
2 R. A. Sperling, P. Rivera gil, F. Zhang, M. Zanella and W. J. Parak, *Chem. Soc. Rev.*, 2008, **37**, 1896–1908.
3 X. Fan, H. Chen, Y. Ding, P. K. Plucinski and A. A. Lapkin, *Green Chem.*, 2008, **10**, 670–677.
4 A. R. Tao, S. Habas and P. D. Yang, *Small*, 2008, **4**, 310–325.
5 Y. Xia, Y. J. Xiong, B. Lim and S. E. Skrabalak, *Angew. Chem., Int. Ed.*, 2009, **48**, 60–103.
6 Lung-Hsin Hung and A.P. Lee, *J. Med. Biol. Eng*, 2007, **27**, 1–6.
7 J. Wagner, T. Kirner, G. Mayer, J. Albert and J.M. Köhler, *Chem. Eng. J.*, 2004, **101**, 251–260.
8 X. Z. Lin, A. D. Terepka and Y. Hong, *Nano Lett.*, 2004, **4**, 2227–2232.
9 S. A. Khan, A. Gunther, M. A. Schmidt and K. F. Jensen, *Langmuir*, 2004, **20**, 8604–8611.
10 J. Wagner and J. M. Kohler, *Nano Lett.*, 2005, **5**, 685–691.
11 D. Shalom, R. C. R. Wootton, R. F. Winkle, B. F. Cottam, R. Vilar, A. J. deMello and C. P. Wilde, *Mater. Lett.*, 2007, **61**, 1146–1150.
12 (*a*) B. K. H. Yen, N. E. Stott, K. F. Jensen and M. G. Bavendi, *Adv. Mater.*, 2003, **15**, 1858–1862; (*b*) M. Kawa, H. Morii, A. Ioku, S. Saita and K. Okuyama, *J. Nanopart. Res.*, 2003, **5**, 81–85.
13 J.M. Köhler, H. Romanus, U. Hübner and J. Wagner, *J. Nanomater.*, 2007, **2007**, 1–7.
14 J.M. Köhler, L. Abhamane, J. Wagner, J. Albert and G. Mayer, *Chem. Eng. Sci.*, 2008, **63**, 5048–5055.
15 W. B. Lee, C. H. Weng, F. Y. Cheng, C. S. Yeh, H. Y. Lei and G. B. Lee, *Biomed. Microdevices*, 2009, **11**, 161–171.
16 Y. J. Song, H. Modrow, L. L. Henry, C. K. Saw, E. E. Doomes, V. Palshin, J. Hormes and C. S. S. R. Kumar, *Chem. Mater.*, 2006, **18**, 2817–2827.
17 S. T. He, Y. L. Liu and H. Maeda, *J. Nanopart. Res.*, 2008, **10**, 209–215.
18 J. L. Huang, L. Q. Lin, Q. B. Li, D. H. Sun, Y. P. Wang, Y. H. Lu, N. He, K. Yang, X. Yang, H. X. Wang, W. T. Wang and W. S. Lin, *Ind. Eng. Chem. Res.*, 2008, **47**, 6081–6090.
19 A. Abou-Hassan, O. Sandre, V. Cabuiland and P. Tabeling, *Chem. Commun.*, 2008, 1783–1785.
20 A. K. Johann Boleininger, Valerie Reuss and Carsten Sonnichsen, *Phys. Chem. Chem.Phys.*, 2006, **8**, 3824–3827.
21 C. H. Weng, C. C. Huang, C. S. Yeh, H. Y. Lei and G. B. Lee, *J Micromech. Microeng*, 2008, 1–8.
22 C. Wu and T. Zeng, *Chem. Mater.*, 2006, **19**, 123–125.
23 (*a*) S. A. Khan and K. F. Jensen, *Adv. Mater.*, 2007, **19**, 2556–2560; (*b*) A.A. Hassan, R. Bazzi and V. Cabuil, *Angew. Chem., Int. Ed.*, 2009, **48**, 7180–7183.
24 K. Geyer, J. D. C. Codee and P. H. Seeberger, *Chem.–Eur. J.*, 2006, **12**, 8434–8442.
25 V. Hessel and H. Lowe, *ACS Symp. Ser.*, 2005, **914**, 23–46.
26 (*a*) A. Kumar, P. K. Vemula, P. M. Ajayan and G. John, *Nat. Mater.*, 2008, **7**, 236–241; (*b*) S. Singh, S. Jaisawal, P. Patel, A. A. Prabhune, C. V. Ramana and B. L. V. Prasad, *New J. Chem.*, 2009, **33**, 646–652.
27 S. R. Emory and S. M. Nie, *Anal. Chem.*, 1997, **69**, 2631–2635.
28 N. A. Inge, V. Bogaert, K. Saerens, C. De Muynck, D. Develter, W. Soetaert and E. J. Vandamme, *Appl. Microbiol. Biotechnol.*, 2007, **76**, 23–34.
29 S. Shah and A. Prabhune, *Biotechnol. Lett.*, 2007, **29**, 267–272 (The oliec acid sophorolipid was synthesized by the growing the candida bombicola in MGYP medium under shaking conditions. To the biomass obtained by centrifugation 2 ml of Oliec acid and 100 ml of 10% glucose solutions were added and incubated at 30 °C for 96 h the viscous solution obtained was separated and purified.).
30 M. B. Kasture, P. Patel, A. A. Prabhune, C. V. Ramana, A. A. Kulkarni and B. L. V. Prasad, *J. Chem. Sci.*, 2008, **120**, 515–520.
31 (*a*) J. Park, J. Joo, G.S. Kwon, Y. Jang and T Hyeon, *Angew. Chem., Int. Ed.*, 2007, **46**, 4630–4660; (*b*) D. Li and R.B. Kaner, *J. Am. Chem. Soc.*, 2006, **128**, 968–975.
32 C. L. de Ligny, in *Adv. Chrom* Vol. 14, pp. 265-304 (1976) (edited by J.C. Giddings, E. Grushka, J. Cazes & P.R. Brown, Marcel Dekker, New York).
33 A. G. Brian, K. H. Yen Martin, A. Schmidt, Klavs F. Jensen and Moungi G. Bawendi, *Angew. Chem., Int. Ed.*, 2005, **44**, 5447–5451.
34 K. L. Kelly, E. Coronado, L. L. Zhao and G. C. Schatz, *J. Phys. Chem. B*, 2003, **107**, 668–677.
35 A. A. S. Bhagat, S. S. Kuntaegowdanahalli and I. Papautsky, *Lab Chip*, 2008, **8**, 1906–1914.